A Recurrent Neural Network Model Accounts for Both Timing and Working Memory Components of an Interval Discrimination Task

Rehan B. Chinoy, Ashita Tanwar and Dean V. Buonomano[*]

Departments of Neurobiology and Psychology, Brain Research Institute, and Integrative Center for Learning and Memory, University of California, Los Angeles, CA 90095–1763, USA

[*]Corresponding author; e-mail: dbuono@ucla.edu

Abstract

Interval discrimination is of fundamental importance to many forms of sensory processing, including speech and music. Standard interval discrimination tasks require comparing two intervals separated in time, and thus include both working memory (WM) and timing components. Models of interval discrimination invoke separate circuits for the timing and WM components. Here we examine if, in principle, the same recurrent neural network can implement both. Using human psychophysics, we first explored the role of the WM component by varying the interstimulus delay. Consistent with previous studies, discrimination was significantly worse for a 250 ms delay, compared to 750 and 1500 ms delays, suggesting that the first interval is stably stored in WM for longer delays. We next successfully trained a recurrent neural network (RNN) on the task, demonstrating that the same network can implement both the timing and WM components. Many units in the RNN were tuned to specific intervals during the sensory epoch, and others encoded the first interval during the delay period. Overall, the encoding strategy was consistent with the notion of mixed selectivity. Units generally encoded more interval information during the sensory epoch than in the delay period, reflecting categorical encoding of short versus long in WM, rather than encoding of the specific interval. Our results demonstrate that, in contrast to standard models of interval discrimination that invoke a separate memory module, the same network can, in principle, solve the timing, WM, and comparison components of an interval discrimination task.

Keywords

computational models, interstimulus interval, interval discrimination, RNNs, working memory

1. Introduction

> *Time and space are the fundamental dimensions of our existence. Although space is gradually losing its value in a world of computer networks, cellular phones and virtual libraries, time is becoming the essence of our times, as is reflected by ever increasing speed, rate of return and productivity – concepts that are intrinsically related to time.*
>
> Buhusi and Meck, 2005

Over the past few decades, it has become increasingly clear that we cannot understand the brain without understanding how the brain tells and represents time. Consequently, neuroscientific and psychological studies of time have expanded dramatically in recent decades. The widespread recognition of the importance of the problem of time and the growth of the timing field is Warren Meck's legacy. In addition to his long list of scientific contributions to the field of timing, he fostered interest in the problem of time and nurtured the generation of scientists responsible for driving the expansion of the timing field.

We now understand that the problem of time is not a single problem, but many interrelated problems (Meck & Ivry, 2016). Here, as scientists that have been influenced by Warren Meck's legacy, we focus on one of these subproblems: interval discrimination on the subsecond scale. Interval discrimination on a subsecond scale is of fundamental importance to sensory processing across the animal kingdom, ranging from communication in crickets, electric fish and frogs, echolocation in bats, and speech, music, and Morse code in humans (Bueti & Buonomano, 2014; Covey & Casseday, 1999; Doupe & Kuhl, 1999; Matthews & Meck, 2016; Motanis et al., 2018; Rose, 2014). In a standard two-interval forced-choice (2IFC) interval discrimination task, subjects first listen to an interval bounded by two tones and, after an interstimulus delay, a second comparison interval is presented, following which subjects must make a judgment as to whether the first or second interval was longer (Bueti & Buonomano, 2014). While there are several variants of the task, this 2IFC format generally requires a working memory component to store the first interval for comparison with the second. This working memory component and the interaction between timing and memory has generally not been a focus of interval discrimination studies. Here we take steps in that direction by using human psychophysics to explore the effects of the delay on interval discrimination performance and develop a recurrent neural network (RNN)-based computational model that performs both the timing and working memory components of the 2IFC interval discrimination task.

A number of different models have been put forth regarding how the brain may tell time in the subsecond range, including pacemaker-accumulators, ramping activity, the oscillator based beat-frequency model, neural population clocks, and

state-dependent network models (Balci & Simen, 2016; Buhusi & Meck, 2005; Buhusi et al., 2016; Creelman, 1962; Gibbon et al., 1984; Gupta et al., 2022; Mauk & Buonomano, 2004; Meck, 1996; Merchant et al., 2013; Paton & Buonomano, 2018; Treisman, 1963). Among these, the state-dependent network (SDN) model, which is constrained to the subsecond range, has made specific predictions regarding the importance of the interstimulus interval, or what can be considered the WM epoch. As originally proposed, time-varying changes in network state produced by neuronal and synaptic properties, such as short-term synaptic plasticity, changed the hidden state of a network (that is, in the absence of ongoing neural activity) in a manner that allowed networks to respond to stimuli in a time-dependent manner (Buonomano, 2000; Buonomano & Merzenich, 1995; Karmarkar & Buonomano, 2007). An early prediction of the SDN model was that short interstimulus delays or the presence of cross-trial temporal uncertainty would degrade performance because the network would not have time to reset to the same baseline state between the first and second intervals. A number of studies have tested these predictions, for example, by using short interstimulus delays between the first and second stimuli and have generally concluded that, at least for very short intervals, e.g., below 300 ms, predictions of the SDN model generally hold true (Buonomano et al., 2009; Fornaciai et al., 2018; Karmarkar & Buonomano, 2007; Sadibolova et al., 2021; Spencer et al., 2009).

In varying the delay between the intervals being discriminated, these studies are potentially also varying the working memory requirements of the task – i.e., the amount of time available to store interval information and the amount of time this information must be stored for. It is unlikely that the decreased performance observed for short interstimulus delays is produced because there is too little time to store the intervals in working memory because, as predicted by the SDN model, if the first and second intervals are presented at different auditory frequencies or visual locations, short interstimulus intervals do not impair performance (Buonomano et al., 2009; Fornaciai et al., 2018; Karmarkar & Buonomano, 2007).

The SDN model, however, does not address the problem of working memory – the transient storage of the first interval – or the mechanisms that underlie how the first and second interval are compared. Early models of timing, however, explicitly invoked distinct circuits for the storage and comparison of the intervals. For example, scalar timing models hypothesized a distinct memory module for storing the reference interval and a comparator circuit which ultimately drove the behavioral response (Gibbon, 1991; Gibbon et al., 1997; Matell & Meck, 2000; Meck, 1996). While these modules were often embedded within a neuroanatomical framework, they did not provide neurobiological interpretations for how these functions were performed.

Here we first examined not only the effects of short interstimulus delays, but also the effects of long interstimulus delays on interval discrimination. We also examined the effects of the order of the short, medium, and long delay blocks

on performance. We show that while performance is strongly affected by short delays, performance for the medium and long delays was similar. This result suggests that, consistent with standard models of working memory, interval information might be stored in steady-state activity during the delay period (Curtis & D'Esposito, 2003; D'Esposito & Postle, 2015; Wang, 2001). Because some brain areas, most notably the prefrontal cortex, have been implicated in some forms of timing (Bakhurin et al., 2017; Emmons et al., 2017; Kim et al., 2013; Oshio et al., 2008; Xu et al., 2014) and working memory (D'Esposito & Postle, 2015; Funahashi et al., 1989; Quintana & Fuster, 1992; Stokes, 2015), we trained a supervised RNN on the same task used in the human studies. Analyses of the RNN showed that units can encode sensory, timing, and working memory components and that, consistent with the notion of mixed selectivity (Buonomano & Maass, 2009; Fusi et al., 2016; Rigotti et al., 2013; Xie et al., 2022) some units could encode more than one feature of the task.

2. Materials and Methods

2.1. Subjects

Subjects consisted of 18 paid individuals (13 females) between the ages of 18 and 39 years. The participants provided written informed consent prior to the experiment and were compensated monetarily for their participation (US$ 8), supplemented with a bonus (US$ 7) if the percentage of correct responses exceeded 65%. The study was approved by the Institutional Review Board at the University of California, Los Angeles, USA. No participants reported having any previous experience in psychoacoustic or interval discrimination tasks from our research lab.

All participants were recruited through Prolific (www.prolific.co), an online data collection service, and reported residency in the United States and fluency in English. The experiment was hosted by Gorilla (www.gorilla.sc), an online experiment builder (Anwyl-Irvine et al., 2021). For consistency and precision purposes, participants were not allowed to complete the experiment using mobile phones or tablets and were limited to the Chrome and Firefox browsers.

Acceptance criteria for inclusion required subjects to have at least 65% accuracy for each experimental condition. Consistent with the increased variability of online psychophysical studies, there was a significant drop-out rate. Of the 32 participants that completed the online study, 18 met criteria. Six of the 14 participants that did not meet criteria were excluded solely based on the performance on the 250-ms condition. Thus, our reported discrimination performance estimates

on the 250-ms condition are likely an overestimation. Initial target enrollment was based on a related pilot experiment study examining timing and working memory.

2.2. Experiment

Participants performed an auditory discrimination task consisting of nine blocks, split into sets of three for each experimental condition. Each set was characterized by three blocks of 80 trials, each with the same interstimulus delay type (experimental condition): 250, 750, or 1500 ms. Participants were randomly assigned the order in which the experimental conditions appeared, counterbalanced across the six possible presentation orders (250-750-1500, 250-1500-750, 750-250-1500, 750-1500-250, 1500-250-750, and 1500-750-250). Additionally, participants had the option to take a brief break between blocks.

Each trial began with an intertrial interval (ITI) sampled from a uniform distribution between 1 and 1.5 seconds. Following the ITI, subjects were presented with two auditory intervals. Each interval was bounded by two 15-ms tone pips of 1 kHz with 5 ms on and off ramps – all stimuli were generated in MATLAB (www.mathworks.com) and uploaded to Gorilla. The interval was measured from the offset of the first tone to the onset of the second. These stimuli were separated by an interstimulus delay period corresponding to the experimental condition of either 250, 750, or 1500 ms. The delay period for each trial was sampled from a uniform distribution between delay ± 0.25× delay. The temporal jitter of the delay introduced temporal uncertainty and eliminates the introduction of a fixed time interval that could potentially be used as a reference to perform the task.

To ensure temporal uncertainty (i.e., that the state of the network at the onset of the second interval was variable), the standard stimulus could be presented first or second and the delays themselves were jittered ±25%. The three delays were presented in consecutive blocks and presentation order was counterbalanced across subjects.

In order to use the same task for the human psychophysics experiments and the RNN simulations, we used the method of constant stimuli rather than an adaptive method (Lapid et al., 2008). Each pair of intervals included a standard interval of 200 ms and a comparison interval of 120, 160, 180, 190, 210, 220, 240, or 280 ms. Each block contained 10 trials of each comparison interval, presented in random order. Subjects were asked to click a button to indicate whether the second stimulus was shorter or longer than the first. Visual feedback was presented immediately after an incorrect response.

2.3. Analysis

The interval discrimination threshold and the point of subjective equality (PSE) were estimated by fits to the logistic function (Lapid et al., 2008):

$$f(x) = \frac{1}{1 + e^{\frac{(x_0 - x)}{k}}}$$

where x_0 and k correspond to the PSE and discrimination threshold (difference limen).

Statistical analyses relied on one-way repeated-measures ANOVAs and post-hoc tests for all analyses were conducted as multiple comparisons using a Tukey–Kramer critical value. We used the ANOVAN and MULTCOMPARE MATLAB functions for these analyses.

2.4. RNN Simulations

2.4.1. Network Structure

Each RNN contained N_{rec} = 256 units, with 204 excitatory and 52 inhibitory units. Before time discretization, the network activity, represented by the vector r, followed a continuous dynamical equation (Yang et al., 2019):

$$\frac{\tau \mathrm{d}r}{\mathrm{d}t} = -r + f\left(W^{\mathrm{rec}}r + W^{\mathrm{in}}u + b + \sqrt{2\tau\sigma_{\mathrm{rec}}{}^2}\xi\right)$$

In this equation, τ = 50 ms represents the neuronal time constant, u is the input to the network, b is the bias or background input, $f(\cdot)$ is the activation function, ξ are N_{rec} independent Gaussian white-noise processes with zero mean and unit variance and σ_{rec} = 0.05 is the strength of the noise. W^{in} and W^{rec} represent the input and recurrent weight matrices, respectively. The activation function f was a standard ReLU function:

$$f(x) = \max(x, 0)$$

An output unit z provided a linear readout of the network: $z = W^{\mathrm{out}}r$.

After using a first-order Euler approximation with a time-discretization step Δt, we have:

$$r_t = (1 - \alpha)r_{t-1} + \alpha f(W^{\mathrm{rec}}r_{t-1} + W^{\mathrm{in}}u_t + b + \sqrt{2\alpha^{-1}\sigma_{\mathrm{rec}}{}^2}N(0,1)$$

where $\alpha = \Delta t / T$, and $N(0,1)$ represents the standard normal distribution. We used a discretization step of Δt = 10 ms, thus α = 0.2.

The input, u, is composed of one input channel that feeds into the recurrent layer. $U = 0$ in the absence of a stimulus and $U = 2$ in the presence of a stimulus. Each interval was demarcated by two 'tones' of 20 ms each. Noise was added to the input channel, so $u = U + u_{\mathrm{noise}}$, where $u_{\mathrm{noise}} = \sigma_u N(0,1)$ and σ_u = 0.005.

2.4.2. Training Procedure

The loss L_{mse} to be minimized was computed by time-averaging the squared errors between the network output $z(t)$ and the target output $\hat{z}(t)$:

$$L_{\mathrm{mse}} = m_t(z_t - \hat{z}_t)^2$$

The squared errors at different time points were differentially weighted by a non-negative mask matrix m_t. Before the response epoch, $m_t = 1$. During the first 50 ms of the response epoch, there was a 'grace period' of $m_t = 0$, while for the rest of the response epoch, $m_t = 2$. We also included an L2 regularization on rates:

$$L_{\mathrm{L2}} = \beta \frac{1}{N_{\mathrm{rec}}} \sum_{i,t} (r_{i,t})^2$$

where we chose $\beta = 10^{-6}$. Thus, the total loss to be minimized was:

$$L = L_{\mathrm{mse}} + L_{\mathrm{L2}}$$

W^{rec} was initialized as a random orthogonal matrix with a gain of 0.1. Next, Dale's was applied by:

$$W^{\mathrm{rec}}_{\mathrm{init}} = DA \left| W_{\mathrm{ortho}} \right|$$

where D is a diagonal matrix composed of +1 or –4, representing excitatory and inhibitory units, respectively. The inhibitory weights were multiplied by a factor of four (the excitatory/inhibitory ratio) to start in a balanced excitatory/inhibitory regime. A is the autapse mask, composed of ones everywhere except a diagonal of zeros imposing no self-connections. $\left| W_{\mathrm{ortho}} \right|$ is the absolute value of the initial orthogonal recurrent weight matrix.

Both recurrent and output weights were trained. Recurrent biases and output biases were initialized to be zero. The input weights, recurrent biases, and output biases were not trained. Training was performed with Adam, a learning rate of 0.001, and the decay rate for the first and second moment estimates were 0.9 and 0.999, respectively. We trained each network for 4000 epochs of 400 trials segmented into 20 batches of 50 trials. The network and the training were implemented in TensorFlow.

2.4.3. 2IFC Interval Discrimination Task and Performance

The 2IFC interval discrimination task used to train the RNN was based on the human psychophysical task (see above) and included a standard interval of 200 ms and comparison intervals of 120, 160, 180, 190, 210, 220, 240, and 280 ms. The delay period was from the onset of the second tone of the first interval to the onset

of the first tone of the second interval. Finally, the response epoch was measured from the onset of the second tone to the end of the trial. For non-response trials (second interval short), if the network responded above a predefined threshold at any point during the trial, the trial was considered an incorrect response. For response trials (second interval long), the network was required to respond above threshold during the response epoch; if it failed to respond during this epoch, or responded at any other time, the trial was considered incorrect.

2.4.4. Interval Tuning

To quantify interval tuning, we used a sensory epoch defined by a window 50 ms before to 50 ms after the offset of the first interval across trials for each first interval condition, and a WM epoch defined by the last 200 ms of the delay period. To focus on the most active units, we used the top quartile of units based on maximum activity during the sensory epoch and separately for the WM epoch. For each unit, the average activity within an epoch was normalized by its maximal activity.

2.4.5. Mutual Information

To calculate the mutual information (MI) for each unit, we first discretized the mean analog rate values into ten bins, ranging from 0 to the maximal value for that unit. We then calculated the MI for unit i as (Buonomano, 2005):

$$MI_i = H(R_i) + H(\text{Int}) - H(R_i, \text{Int})$$

where $H(R_i)$ is the conventional entropy measure of the binned activity. $H(\text{Int})$ reflects the entropy of the interval distribution, which was equiprobable (1/9). $H(R_i, \text{Int})$ is the joint entropy.

3. Results

3.1. Effect of the Interstimulus Delay on Performance

To study the effect of short and long interstimulus delays on interval discrimination, we used an auditory 2IFC task with a standard interval of 200 ms (see section 2, *Methods*). Three delay conditions were examined: 250, 750, and 1500 ms (Fig. 1A). There was an overall effect of delay on the interval discrimination threshold but not on the point of subjective equality (Fig. 1B–D). Specifically, a one-way ANOVA revealed a significant effect of delay ($F_{2,34} = 12.42$, $p < 10^{-4}$, $\eta^2 = 0.18$), and a multiple-comparison analysis confirmed that the threshold in the 250 ms condition was significantly higher than in the 750 and 1500 ms conditions ($p < 0.001$). These results are consistent with previous studies that reported that a 250-ms interstimulus delay impairs interval discrimination of 100 and 200 ms standards (Karmarkar & Buonomano, 2007; Sadibolova et al., 2021), and establish that there is no negative impact of long delays potentially causing degradation of information in WM.
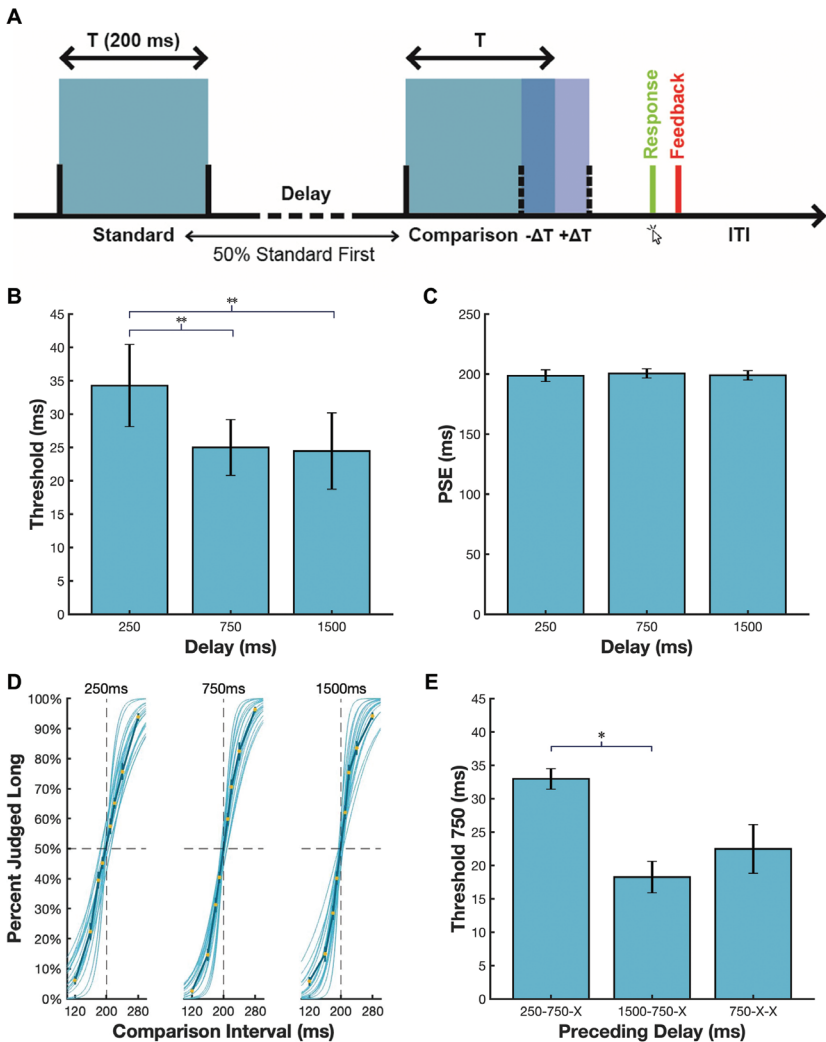
Figure 1. Psychophysics. (A) Schematic illustration of the task. Each trial consisted of two auditory intervals bounded by 15 ms tones (standard interval = 200 ms). The interstimulus delay was either 250 ms, 750 ms, or 1500 ms. Participants responded by indicating whether the second interval was shorter or longer than the first. (B) Threshold data for all participants by delay condition. The interval discrimination threshold was significantly higher for the 250 ms interstimulus delay condition compared to the 750 and 1500 ms conditions ($p < 0.01$). There was no significant difference between the 750 and 1500 ms condition. (C) Point of subjective equality (PSE) data for all participants. There was no significant difference between the average PSE between the three delay types. (D) Fitted individual psychometric functions for all 18 subjects on the 250 ms, 750 ms, and 1500 ms delay conditions. The average R^2 values of the fits were 0.93 ± 0.0084, 0.96 ± 0.0082, and 0.96 ± 0.0093, for the 250, 750, and 1500 ms conditions, respectively. The means and SEM are shown in overlay. (E) Threshold data for the 750 ms delay condition separated by whether it was preceded by a 250 ms block, a 1500 ms block, or no blocks. A significant increase in threshold for the 750 ms delay condition was observed when it was preceded by the 250 ms delay condition ($p < 0.05$).

We also examined whether there was any short-term learning or adaptation effect by asking whether performance for a 750 ms delay was influenced by the delay that preceded it (Fig. 1E). A one-way analysis of variance on the threshold of the 750 ms delay across conditions in which the 750 ms block came after the 250 or 1500 ms blocks, or was the first block, revealed a small but significant effect ($F_{2,8} = 4.5$, $p < 0.05$, $\eta^2 = 0.53$). This effect was driven by the condition in which the 750 ms delay was preceded by 250 ms block. Because the 250 ms delay is significantly harder, this result is consistent with the notion that perceptual learning benefits from exposure to easier stimuli first (Ahissar & Hochstein, 2004). However, we stress that because of the number of order conditions, analyses of any order effects are underpowered.

3.2.   A RNN Model of Interval Discrimination

Artificial neural networks and supervised RNNs in particular have proven to be a valuable tool toward understanding how neural circuits perform an array of different computations (Chaisangmongkon et al., 2017; Kim & Sejnowski, 2021; Laje & Buonomano, 2013; Mante et al., 2013; Yang & Wang, 2020). But as far as we are aware, RNN models of 2IFC interval discrimination that include both a timing and working memory component have not been developed. Thus, we explored if it is possible for a single recurrent circuit to perform this task and, if so, how time is both discriminated and stored in WM (Fig. 2A). For biological plausibility, the RNN consisted of subpopulations of excitatory and inhibitory units (see section 2, *Methods*).

The RNN task closely matched the psychophysical interval discrimination task. Initially, the RNN was trained with a standard interval of 200 ms and a delay of 750 ms. The comparison intervals were 120, 160, 180, 190, 210, 220, 240, or 280 ms, and the presentation order of the standard and comparison intervals were randomized. Training and testing were performed on all comparison intervals.

After training, the performance of five RNNs was near perfect at the trained 750 ms delay (Fig. 2B). That is, almost all trials with a short comparison interval were classified as short (no output response) and trials with long comparison intervals were classified as long (output response). Next, these RNNs were tested on the same task but with interstimulus delays of 250 or 1500 ms. Performance was not significantly decreased for the 1500 ms delay compared to the 750 ms delay but was dramatically worse for the 250 ms delay ($p < 0.01$): percent correct performance was approximately 66%. The decreased performance mirrors the prediction of the SDN model because the RNN has not stabilized or reset into a consistent network state at the onset of the second interval. Importantly, however, in the absence of short-term synaptic plasticity (which was not incorporated into the model), this RNN does not explicitly test prediction of the SDN model and confounds potential state-dependent effects and the time it takes the RNN to 'store' a memory of the first interval. The generalization from 750 to 1500 ms

indicates that information about the duration of the first interval is stored over the delay period as a fixed-point attractor in which the activity of the units is not changing significantly.
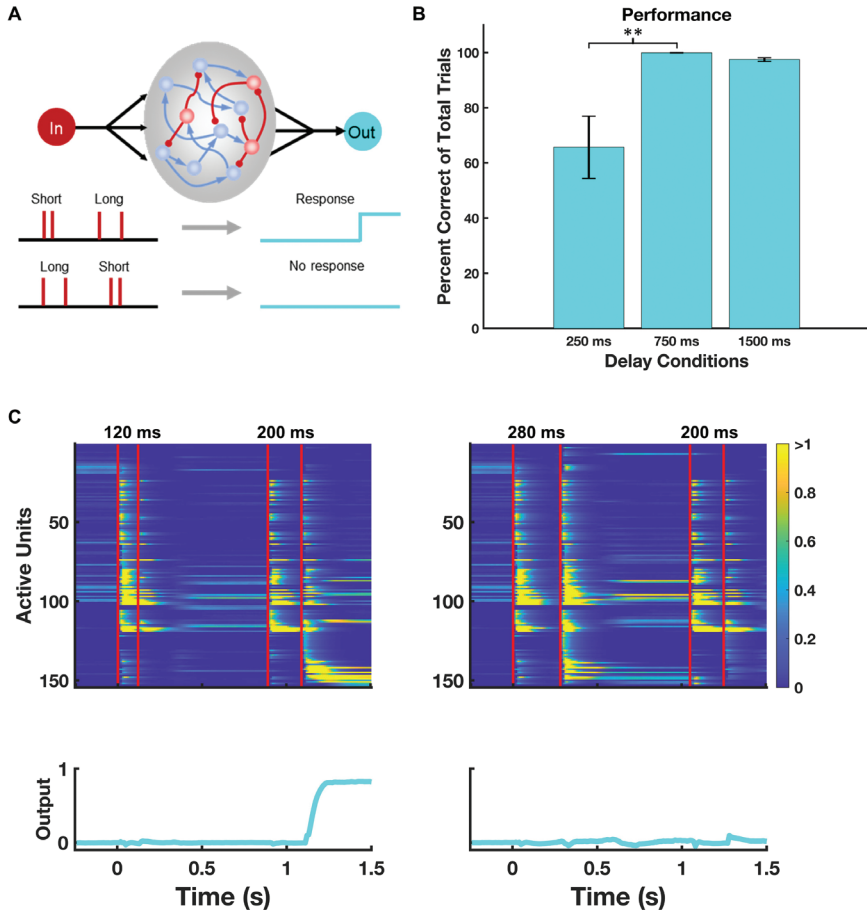
Figure 2. (A) Schematic of the recurrent neural network (RNN) model. The input unit projects to the RNN composed of 256 units (204 excitatory, 52 inhibitory). The recurrent units project to the output unit. The network is trained to produce a motor response for trials in which the second interval is longer than the first interval following the offset of the second interval. (B) Performance. Percent correct trials for five networks on three different delay conditions. Networks were trained on the 750 ms condition. There was a significant decrease in performance in the 250 compared to the 750 ms condition. ($p < 0.01$, Wilcoxon rank-sum test). (C) Sample population activity of a trained RNN tested on two different trial conditions. Red bars indicate input pulses. Left panel shows network activity for the short interval (120 ms) followed by the standard interval (200 ms) case, and right panel shows network activity for the long-standard case. For visualization purposes, only units with a peak activity of over 0.1 on any trial are displayed. Cyan plots represent activity of the output unit.

3.3. Mechanisms Underlying Timing and WM in the RNN

The overall dynamics of all the active units of one RNN in response to a short–long (120–200 ms) and a long–short (280–200) trial are shown in Fig. 2C. Units are sorted according to the latency of their peak response. We can see that most cells have properties of sensory units, in that they respond to both the first and second 'tone' of the first and second intervals. But it is also possible to see that the response to each tone is modulated by temporal context and that some units are active during an interval (i.e., during the intertone interval).

Within-interval activity is ultimately responsible for timing, i.e., for implementing a timer. Specifically, timing of an interval requires a trace or memory of the first tone, which affects the response of the second tone. There are two general mechanisms by which neural circuits can maintain information about the past: in the hidden or active state of a network (Buonomano & Maass, 2009). The hidden state includes short-term synaptic plasticity, and the active state consists of ongoing suprathreshold neural activity. In the absence of short-term synaptic plasticity, the temporal information is maintained in the active state. Note that, in principle, the hidden state also includes the membrane time constant – here, however, with τ = 50 ms, passive decay should not significantly contribute to the timing of intervals of 200 ms.

We can also see that population activity decreases dramatically during the interstimulus delay. But critically, a small subset of units maintained an approximately constant level of activity during the latter part of the delay and this activity was dependent on the duration of the first interval. These units are encoding the WM of the first interval.

To better understand the timing and WM mechanisms of the RNN, it is useful to look at the activity of sensory, interval-tuned, and WM units across all trial types. Figure 3A shows an example of a 'pure' sensory unit in which the response to each tone of each interval is approximately the same – i.e., independent of the interval. Figure 3B provides an example of an interval-tuned inhibitory unit that, at the offset of the second tone, responds more to the longer intervals. This unit has mixed selectivity properties because it also encodes (at a lower activity rate) long intervals during the WM epoch. Figure 3C shows a WM neuron that fires tonically during the latter half of the delay period. Importantly, it fires at a higher rate when the first interval was short and approximately the same amount regardless of whether the first interval was 120, 140, 160, or 180 ms. This neuron is thus storing WM critical to the task, rather than the precise duration of the first interval. In essence, it is categorically encoding whether the first interval was short or long. Figure 3D provides an example of a 'pure' interval-tuned unit that displays its tuning primarily during the sensory epoch, responding more at the offset of longer intervals.
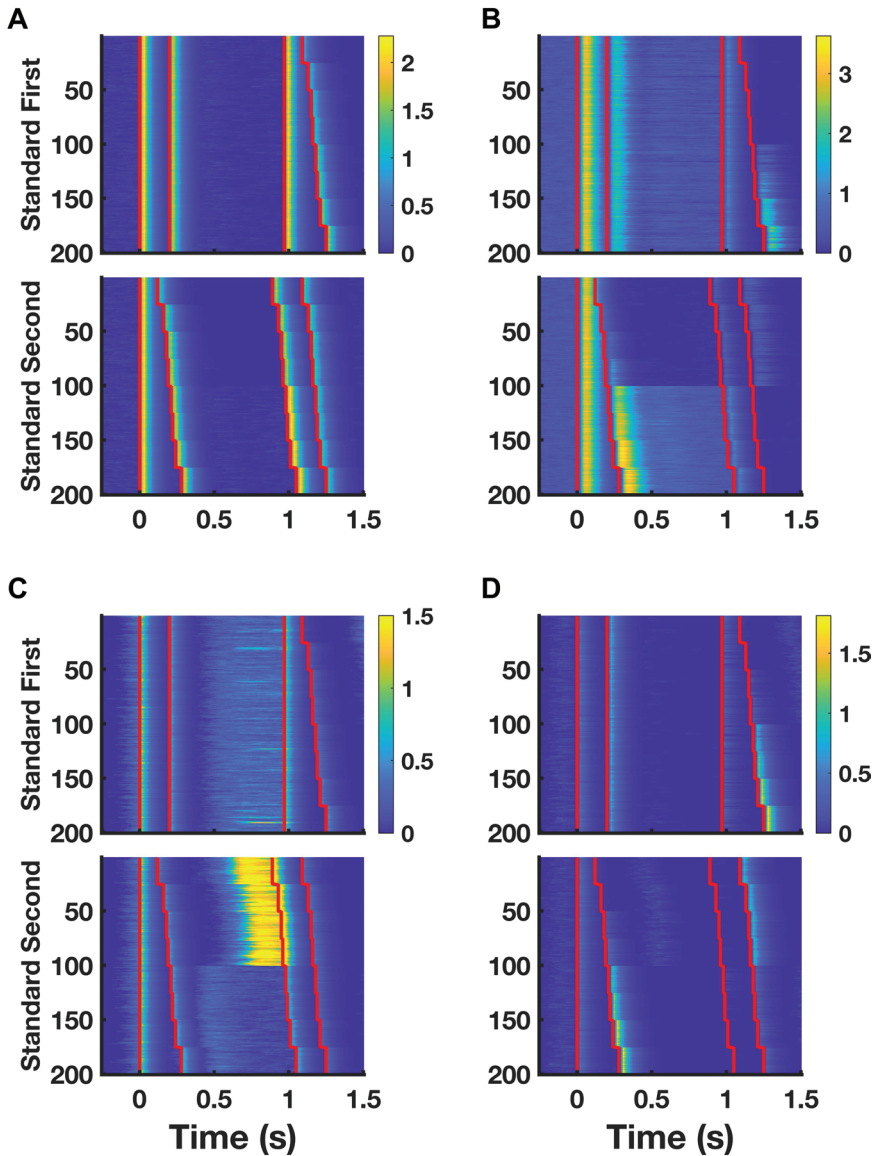
Figure 3. Four example recurrent neural network (RNN) units. For each panel, the top plot shows activity for trials in which the standard interval (200 ms) is shown first, and the bottom plot shows activity for trials in which the standard is second. (A) A sensory unit that responds consistently to each input pulse. (B) An interval-tuned unit that exhibits progressively stronger responses to longer intervals. The unit also encodes long intervals during the WM epoch. (C) WM unit that exhibits approximately categorical response to short-first intervals. (D) Interval-tuned unit that preferentially responds to long intervals during the sensory epoch.

3.4. *Mixed Selectivity of Interval Tuning and Interval Storage in WM*

The notion of mixed selectivity reflects experimental and computational observations that, within recurrent circuits, neurons often contribute to more than one computational component of a task (Buonomano & Maass, 2009; Fusi et al., 2016; Rigotti et al., 2013). We next determined if units in the RNN exhibit mixed selectivity, i.e., if they multiplexed timing and WM. We first examined interval selectivity during the sensory epoch (a window straddling the offset of the second tone of the first interval) and the end of the delay period (the WM epoch). Figure 4A shows the tuning curves of the active units of one RNN sorted according to which interval elicited the largest response during the sensory epoch. We can see that most units exhibited preferred interval tuning to either the shortest or longest interval and that most units exhibited graded tuning to interval. Figure 4B shows the interval tuning during the last 100 ms of the delay period. The plot reveals that in contrast to the sensory epoch, encoding during the WM epoch was more categorical in nature (Supplementary Fig. S1). Thus, the strategy the RNN took to solve the task was not to store the absolute first interval in WM, but whether it was shorter or longer than 200 ms. In other words, the key computation of whether the first stimulus was short or long was performed before the arrival of the second interval. This observation is consistent with psychophysical studies that suggest that subjects in some cases can make short or long decisions before the arrival of the second interval, and that subjects can perform interval discrimination tasks when only one interval is presented (Buonomano et al., 2009).

To quantify the interval tuning, we calculated the mutual information (MI) each unit contained about the nine possible intervals (max MI = 3.17). This
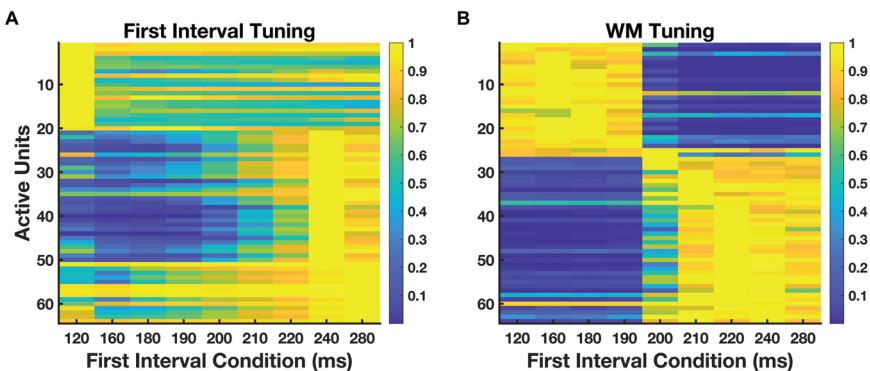

Figure 4. (A) Interval tuning to first interval (sensory epoch). Each row represents a single unit's tuning function across all nine possible first interval conditions during the sensory epoch. The units are sorted in order of preferred interval tuning. Only the top quartile of active units is shown. (B) Interval tuning during the working-memory (WM) epoch. Note that in contrast to interval tuning during the sensory epoch, most units categorically encode short (< 200 ms) or long (>200 ms) intervals.

analysis focused on the units that were most active during either the sensory or WM epochs (see section 2, *Methods*). Overall, units contained significantly more interval information during the sensory epoch compared to the WM epoch ($p < 0.01$) (Fig. 5A, B). To examine whether the units exhibited mixed selectivity, i.e., if they contained interval information during the sensory and WM epochs, we examined a MI scatterplot for all five RNNs (Fig. 5A), which revealed a highly heterogeneous distribution of units. Units primarily encoded a lot of information about the first interval, but little or no interval information during the WM epoch (upper left quadrant). In contrast, other units contained interval information during the WM, but not sensory, epoch (lower right quadrant). Other units contained more interval information during both the sensory and WM epochs (upper right quadrant). Note that the overrepresentation of units with MI $\cong$ 1 bit during the WM epoch reflect the categorical encoding of the binary information: short $\times$ long. The presence of mixed selectivity in the model is consistent with the diversity of neural responses observed in PFC recordings in a nonhuman primate study during a duration discrimination task (Genovesio et al., 2009).

4. Discussion

Interval discrimination tasks often require two distinct computations: the ability to measure elapsed time and the ability to store the first interval for comparison with the second. To date, models of interval discrimination have assumed that interval discrimination and storage of the interval are distinct computations performed by different brain areas. Here we first explored whether the amount
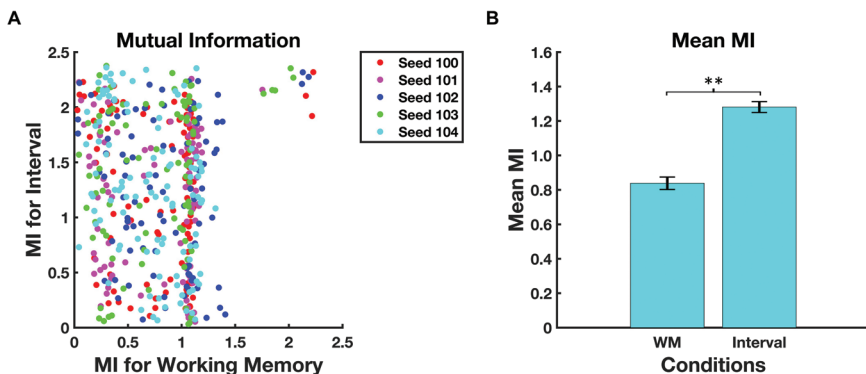
Figure 5. (A) Scatterplot of the mutual information (in bits) that each active unit contains about the nine intervals during the sensory and working-memory (WM) epochs. Note that the overrepresentation of WM mutual information (MI) values that approximate 1 reflect the categorical encoding of short versus long intervals. (B) Mean mutual information for all data points shown in A. There is significantly greater mutual information during the sensory epoch compared to the WM epoch ($p < 0.01$, Wilcoxon rank-sum test).

of time information required to be stored in WM influences performance, and whether, in principle, the same network can accomplish both the timing and WM components of a 2IFC discrimination task.

4.1. *Interstimulus Delay and Working Memory*

Several studies have explored the role of the interstimulus delay in interval discrimination (Buonomano et al., 2009; Fornaciai et al., 2018; Karmarkar & Buonomano, 2007; Sadibolova et al., 2021). These studies were mostly motivated by the SDN model, which predicts that when there is not enough time for the network state to reset and there is temporal variability across trials, the first and second intervals will interfere with each other because the network will be in different states within each trial. For the most part, studies have confirmed SDN predictions for standard intervals and delays below 300 ms, but there is ongoing debate as to the time scale at which these predictions hold true (Fornaciai et al., 2018; Sadibolova et al., 2021; Spencer et al., 2009).

The interstimulus delay also has important implications in the context of the WM component of interval discrimination. The timing and working memory components of standard interval discrimination tasks have in general been considered to be distinct computations performed by distinct circuits (Meck, 1996). Recent studies, however, have suggested potential links between timing and working memory. For example, psychophysical studies in humans have shown that the temporal structure of tasks is implicitly learned during WM tasks and that WM is impaired when information has to be retrieved at unexpected times (Cravo et al., 2017; Jin et al., 2020; Nobre & van Ede, 2018; van Ede et al., 2017).

Here we analyzed the performance of subjects on a 2IFC discrimination task with a standard interval of 200 ms and explored the effect of short (250 ms), medium (750 ms), and long (1500 ms) interstimulus delays. Our findings again confirm that short delays impair performance. We did not observe any effects of long delays, as there was no significant difference in interval discrimination thresholds between 750- and 1500-ms delays. This result is consistent with the notion that once a memory of the first interval is stored in WM, it is stored as a fixed-point attractor and is thus time-independent.

Following the work of Nobre and colleagues (Cravo et al., 2017; Jin et al., 2020; Nobre & van Ede, 2018; van Ede et al., 2017), future studies should address the question of implicit timing of the interstimulus delay – specifically, whether subjects create an implicit expectation of the duration of the delay during interval discrimination tasks. This question can be addressed by using a 2IFC task with a standard delay interspersed with unexpected shorter or longer interstimulus delays on a small number of trials.

4.2. An RNN Model of Interval Discrimination

Here we presented what is, to the best of our knowledge, the first RNN implementation of a 2IFC interval discrimination task. Our goal was to determine if the timing and WM components of the task could be performed by the same network and, if so, how the units of the RNN accomplished these distinct computations. Our results establish that an RNN can effectively learn the same 2IFC task used in our psychophysical studies. RNNs trained on the 750 ms delay performed the task almost perfectly in terms of percent correct. We did not report the RNN results in terms of their psychophysical thresholds because they are determined primarily by the intervals used during the training – and the threshold can probably be arbitrarily low when an RNN is trained with intervals very close to the standard. When the RNNs trained on the 750 ms delay were tested on the 250 and 1500 ms interstimulus delays, we observed a significantly impaired performance at the 250 ms delay. This result loosely mirrors the impairment at 250 ms in the psychophysical studies. In the RNN, the effect is due to the interference between the first and second interval because the network has not fully converged to steady-state activity during the delay period. Consequently, the categorical tuning to the intervals during the delay epoch was poorer in the 250 ms compared to the 750 ms trials (the R^2 values of the sigmoidal fits were significantly worse for 250 ms trials, $p < 10^{-4}$).

The RNN implemented here, is of course, an impoverished representation of biological networks in that it lacks short-term synaptic plasticity, inhibitory subtypes, interareal interactions, oscillations, and the intrinsic time constants imposed by ion channels and receptor kinetics. Thus, we stress that our model does not comprise a test of the SDN model. But the simplicity of the model allows us to conclude that timing per se must rely on the decay of activity in response to the first tone (characterized by the membrane time constant) and/or the internal dynamics defined by the recurrent connectivity. Reliance on the activity decay is consistent with memory-decay or energy models (Killeen & Grondin, 2021; Rammsayer, 1994; Tiganj et al., 2015), and is likely to be contributing to the timing here. But overall, the presence of sustained activity in some units during the interval (late peak latency) and the fact that the second tone can produce a larger response, indicate that the network is actively using its internal dynamics to tell time – which is consistent with neural population clock models (Buonomano, 2005; Paton & Buonomano, 2018).

A well-defined property of motor and sensory timing is Weber's law; and any biologically plausible model of timing should account for Weber's law. The current model was implemented as a supervised RNN, and consequently, the precision of interval discrimination is largely determined by the intervals chosen by the experimenter during training. Thus, the current framework is not well suited to determine if the model exhibits Weber's law; however, we have previously

shown that similar RNN approaches exhibit Weber's law (Hardy et al., 2018; Laje & Buonomano, 2013).

Both in the context of timing tasks and the wide variety of other psychophysical tasks that rely on working memory, it has generally been assumed that working memory is a distinct computation performed by specific neural circuits. However, converging experimental (Carnevale et al., 2015; Mante et al., 2013; Miller et al., 1996; Rainer et al., 1999) and computational data (Fusi et al., 2016; Goudar & Buonomano, 2018; Mante et al., 2013; Orhan & Ma, 2019; Rigotti et al., 2013; Yang et al., 2019) suggest that the critical computations for a given task (e.g., interval discrimination or motion integration during a random-dot motion task) and WM may be performed and encoded not only with the same circuits, but within the same neurons.

Early models of interval discrimination have invoked three separate computations, each performed by a separate module: a pacemaker responsible for timing per se, a memory module responsible for transiently storing a reference interval, and a comparator responsible for determining whether the current or stored values is larger and thus if the first or second interval is longer (Gibbon, 1991; Gibbon et al., 1997; Matell & Meck, 2000; Meck, 1996). Here we have established that, in principle, a single circuit can perform a 2IFC task and thus all three computations can be performed in a multiplexed fashion by the same group of units.

Key to the ability to perform these three components is the notion of state-dependent computations (Buonomano & Maass, 2009; Goudar & Buonomano, 2018). After each interval, the network converges to a steady-state fixed-point attractor during the delay period, which encodes information about the first interval. This fixed point serves as the starting state at the arrival of the second interval. And depending on the interaction between this starting state and the duration of the second interval, the network generates a short or long response – effectively implementing the comparator function.

Our goal is not to propose that the RNNs simulated here represent a biologically realistic implementation of the 2IFC task. Indeed, consistent with the SDN model of timing, a converging body of data suggests that sensory areas contribute to the timing of intervals on the subsecond scale, and higher-order areas underlie the WM component (Chubykin et al., 2013; Karmarkar & Buonomano, 2007; Monk et al., 2020; Motanis et al., 2018; Namboodiri et al., 2014; Paton & Buonomano, 2018; Shuler & Bear, 2006). Nevertheless, higher-order prefrontal areas have been implicated in both timing (Bakhurin et al., 2017; Emmons et al., 2017; Kim et al., 2013; Oshio et al., 2008; Xu et al., 2014) and working memory (D'Esposito & Postle, 2015; Funahashi et al., 1989; Quintana & Fuster, 1992; Stokes, 2015). Thus, future work should determine if interval discrimination in the subsecond range is performed in a modular fashion, as well as whether, in some cases, the same neural circuits are indeed capable of performing both timing and WM components in a multiplexed fashion. Finally, our results show how the same network can

implement three computations – timing, memory, and comparison – that were previously proposed to be performed by three distinct modules.

Acknowledgements

Supplementary Material

Supplementary material is available online at: https://doi.org/10.6084/m9.figshare.20438736

References

Ahissar, M., & Hochstein, S. (2004). The reverse hierarchy theory of visual perceptual learning. *Trends Cogn. Sci.*, *8*, 457–464. doi: 10.1016/j.tics.2004.08.011.

Anwyl-Irvine, A., Dalmaijer, E. S., Hodges, N., & Evershed, J. K. (2021). Realistic precision and accuracy of online experiment platforms, web browsers, and devices. *Behav. Res. Meth.*, *53*, 1407–1425. doi: 10.3758/s13428-020-01501-5.

Bakhurin, K. I., Goudar, V., Shobe, J. L., Claar, L. D., Buonomano, D. V., & Masmanidis, S. C. (2017). Differential encoding of time by prefrontal and striatal network dynamics. *J. Neurosci.*, *37*, 854–870. doi: 10.1523/JNEUROSCI.1789-16.2016.

Balcı, F., & Simen, P. (2016). A decision model of timing. *Curr. Opin. Behav. Sci.*, *8*, 94–101. doi: 10.1016/j.cobeha.2016.02.002.

Bueti, D., & Buonomano, D. V. (2014). Temporal perceptual learning. *Timing Time Percept.*, *2*, 261–289. doi: 10.1163/22134468-00002023.

Buhusi, C. V., & Meck, W. H. (2005). What makes us tick? Functional and neural mechanisms of interval timing. *Nat. Rev. Neurosci.*, *6*, 755–765. doi: 10.1038/nrn1764.

Buhusi, C. V., Oprisan, S. A., & Buhusi, M. (2016). Clocks within clocks: timing by coincidence detection. *Curr. Opin. Behav. Sci.*, *8*, 207–213. doi: 10.1016/j.cobeha.2016.02.024.

Buonomano, D. V. (2000). Decoding temporal information: a model based on short-term synaptic plasticity. *J. Neurosci.*, *20*, 1129–1141. doi: 10.1523/JNEUROSCI.20-03-01129.2000.

Buonomano, D. V. (2005). A learning rule for the emergence of stable dynamics and timing in recurrent networks. *J. Neurophysiol.*, *94*, 2275–2283. doi: 10.1152/jn.01250.2004.

Buonomano, D. V., Bramen, J., & Khodadadifar, M. (2009). Influence of the interstimulus interval on temporal processing and learning: testing the state-dependent network model. *Philos. Trans. R. Soc. Lond. B Biol. Sci.*, *364*, 1865–1873. doi: 10.1098/rstb.2009.0019.

Buonomano, D. V., & Maass, W. (2009). State-dependent computations: spatiotemporal processing in cortical networks. *Nat. Rev. Neurosci.*, *10*, 113–125. doi: 10.1038/nrn2558.

Buonomano, D. V., & Merzenich, M. M. (1995). Temporal information transformed into a spatial code by a neural network with realistic properties. *Science*, *267*, 1028–1030. doi: 10.1126/science.786333.

Carnevale, F., de Lafuente, V., Romo, R., Barak, O., & Parga, N. (2015). Dynamic control of response criterion in premotor cortex during perceptual detection under temporal uncertainty. *Neuron*, *86*, 1067–1077. doi: 10.1016/j.neuron.2015.04.014.

Chaisangmongkon, W., Swaminathan, S. K., Freedman, D. J., & Wang, X.-J.(2017). Computing by robust transience: how the fronto-parietal network performs sequential, category-based decisions. *Neuron*, *93*, 1504–1517.e4. doi: 10.1016/j.neuron.2017.03.002.

Chubykin, A. A., Roach. E. B., Bear, M. F., & Shuler, M. G. H. (2013). A cholinergic mechanism for reward timing within primary visual cortex. *Neuron*, *77*, 723–735. doi: 10.1016/j.neuron.2012.12.039.

Covey, E., & Casseday, J. H. (1999). Timing in the auditory system of the bat. *Annu. Rev. Physiol.*, *61*:, 457–476. doi: 10.1146/annurev.physiol.61.1.457.

Cravo, A. M., Rohenkohl, G., Santos, K. M., & Nobre, A. C. (2017). Temporal anticipation based on memory. *J. Cogn. Neurosci.*, *29*, 2081–2089. doi: 10.1162/jocn_a_01172.

Creelman, C. D. (1962). Human discrimination of auditory duration. *J. Acoust. Soc. Am.*, *34*, 582–593. doi: 10.1121/1.1918172.

Curtis, C. E., & D'Esposito, M. (2003). Persistent activity in the prefrontal cortex during working memory. *Trends Cogn. Sci.*, *7*, 415–423. doi: 10.1016/S1364-6613(03)00197-9.

D'Esposito, M., & Postle, B. R. (2015). The cognitive neuroscience of working memory. *Annu. Rev. Psychol.*, *66*, 115–142. doi: 10.1146/annurev-psych-010814-015031.

Doupe, A. J., & Kuhl, P. K. (1999). Birdsong and human speech: common themes and mechanisms. *Annu. Rev. Neurosci.*, *22*, 567–631. doi: 10.1146/annurev.neuro.22.1.567.

Emmons, E. B., De Corte, B. J., Kim, Y., Parker, K. L., Matell, M. S, & Narayanan, N. S. (2017). Rodent medial frontal control of temporal processing in the dorsomedial striatum. *J. Neurosci.*, *37*, 8718–8733. doi: 10.1523/JNEUROSCI.1376-17.2017.

Fornaciai, M., Markouli, E., & Di Luca, M. (2018). Modality-specific temporal constraints for state-dependent interval timing. *Sci. Rep.*, *8*, 10043. doi: 10.1038/s41598-018-28258-4.

Funahashi, S., Bruce, C. J., & Goldman-Rakic, P. S. (1989). Mnemonic coding of visual space in the monkey's dorsolateral prefrontal cortex. *J. Neurophysiol.*, *61*, 331–349. doi: 10.1152/jn.1989.61.2.331.

Fusi, S., Miller, E. K., & Rigotti, M. (2016). Why neurons mix: high dimensionality for higher cognition. *Curr. Opin. Neurobiol.*, *37*, 66–74. doi: 10.1016/j.conb.2016.01.010.

Genovesio, A., Tsujimoto, S., & Wise, S. P. (2009). Feature- and order-based timing representations in the frontal cortex. *Neuron*, *63*, 254–266. doi: 10.1016/j.neuron.2009.06.018.

Gibbon, J. (1991). Origins of scalar timing. *Learn. Motiv.*, *22*, 3–38. doi: 10.1016/0023-9690(91)90015-Z.

Gibbon, J., Church, R. M., & Meck, W. H. (1984). Scalar timing in memory. *Ann. N. Y. Acad. Sci.*, *423*, 52–77. doi: 10.1111/j.1749–6632.1984.tb23417.x.

Gibbon, J., Malapani, C., Dale, C. L., & Gallistel, C. R. (1997). Toward a neurobiology of temporal cognition: advances and challenges. *Curr. Opin. Neurobiol.*, *7*, 170–184. doi: 10.1016/S0959-4388(97)80005-0.

Goudar, V., & Buonomano, D. V. (2018). Encoding sensory and motor patterns as time-invariant trajectories in recurrent neural networks. *eLife*, *7*, e31134. doi: 10.7554/eLife.31134.001.

Gupta, A., Bansal, R., Alashwal, H., Kacar, A. S., Balci, F., & Moustafa, A. A. (2022). Neural substrates of the drift-diffusion model in brain disorders. *Front. Comput. Neurosci.*, *15*, 678232. doi: 10.3389/fncom.2021.678232.

Hardy, N. F., Goudar, V., Romero-Sosa, J. L., & Buonomano, D. V. (2018). A model of temporal scaling correctly predicts that motor timing improves with speed. *Nat. Commun.*, *9*, 4732. doi: 10.1038/s41467-018-07161-6.

Jin, W., Nobre, A. C., & van Ede, F. (2020). Temporal expectations prepare visual working memory for behavior. *J. Cogn. Neurosci.*, *32*, 2320–2332. doi: 10.1162/jocn_a_01626.

Karmarkar, U. R., & Buonomano, D. V. (2007). Timing in the absence of clocks: encoding time in neural network states. *Neuron*, *53*, 427–438. doi: 10.1016/j.neuron.2007.01.006.

Killeen, P. R., & Grondin, S. (2021). A trace theory of time perception. *Psychol. Rev*. doi: 10.1037/rev0000308.

Kim, J, Ghim, J.-W., Lee, J. H., & Jung, M. W. (2013). Neural correlates of interval timing in rodent prefrontal cortex. *J. Neurosci.*, *33*, 13834–13847. doi: 10.1523/JNEUROSCI.1443-13.2013.

Kim, R., & Sejnowski, T. J. (2021). Strong inhibitory signaling underlies stable temporal dynamics and working memory in spiking neural networks. *Nat. Neurosci.*, *24*, 129–139. doi: 10.1038/s41593-020-00753-w.

Laje, R., & Buonomano, D. V. (2013). Robust timing and motor patterns by taming chaos in recurrent neural networks. *Nat. Neurosci.*, *16*, 925–933. doi: 10.1038/nn.3405.

Lapid, E., Ulrich, R., & Rammsayer, T. (2008). On estimating the difference limen in duration discrimination tasks: A comparison of the 2AFC and the reminder task. *Percept. Psychophys.*, *70*, 291–305. doi: 10.3758/PP.70.2.291.

Mante, V., Sussillo, D., Shenoy, K. V., Newsome, W. T. (2013). Context-dependent computation by recurrent dynamics in prefrontal cortex. *Nature*, *503*, 78–84. doi: 10.1038/nature12742.

Matell, M. S., & Meck, W. H. (2000). Neuropsychological mechanisms of interval timing behavior. *BioEssays*, *22*, 94–103. doi: 10.1002/(SICI)1521–1878(200001)22:1 < 94::AID-BIES14>3.0.CO;2-E.

Matthews, W. J., & Meck, W. H. (2016). Temporal cognition: connecting subjective time to perception, attention, and memory. *Psychol. Bull.*, *142*, 865–890. doi: 10.1037/bul0000045.

Mauk, M. D., & Buonomano, D. V. (2004). The neural basis of temporal processing. *Annu. Rev. Neurosci.*, *27*, 307–340. doi: 10.1146/annurev.neuro.27.070203.144247.

Meck, W. H. (1996). Neuropharmacology of timing and time perception. *Cogn. Brain Res.*, *3*, 227–242. doi: 10.1016/0926-6410(96)00009-2.

Meck, W. H., & Ivry, R. B. (2016). Editorial overview: Time in perception and action. *Curr. Opin. Behav. Sci.*, *8*, vi–x. doi: 10.1016/j.cobeha.2016.03.001.

Merchant, H., Harrington, D. L., & Meck, W. H. (2013). Neural basis of the perception and estimation of time. *Annu. Rev. Neurosci.*, *36*, 313–336. doi: 10.1146/annurev-neuro-062012-170349.

Miller, E. K., Erickson, C. A., & Desimone, R.(1996). Neural mechanisms of visual working memory in prefrontal cortex of the macaque. *J. Neurosci.*, *16*, 5154–5167. doi: 10.1523/JNEUROSCI.16-16-05154.1996.

Monk, K. J., Allard, S., Hussain Shuler, M. G. (2020). Reward timing and its expression by inhibitory interneurons in the mouse primary visual cortex. *Cereb. Cortex*, *30*, 4662–4676. doi: 10.1093/cercor/bhaa068.

Motanis, H., Seay, M. J., & Buonomano, D. V. (2018). Short-term synaptic plasticity as a mechanism for sensory timing. *Trends Neurosci.*, *41*, 701–711. doi: 10.1016/j.tins.2018.08.001.

Namboodiri, V. M. K., Mihalasm, S., Marton, T. M. & Hussain Shuler, M. G. (2014). A general theory of intertemporal decision-making and the perception of time. *Front. Behav. Neurosci.*, *8*, 61. doi: 10.3389/fnbeh.2014.00061.

Nobre, A. C., & van Ede, F. (2018). Anticipated moments: temporal structure in attention. *Nat. Rev. Neurosci.*, *19*, 34–48. doi: 10.1038/nrn.2017.141.

Orhan, A. E., & Ma, W. J. (2019). A diverse range of factors affect the *nature*, of neural representations underlying short-term memory. *Nat. Neurosci.*, *22*, 275–283. doi: 10.1038/s41593-018-0314-y.

Oshio, K., Chiba,A,. & Inase, M. (2008). Temporal filtering by prefrontal neurons in duration discrimination. *Eur. J. Neurosci.*, *28*, 2333–2343. doi: 10.1111/j.1460-9568.2008.06509.x.

Paton, J. J., & Buonomano, D. V. (2018). The neural basis of timing: distributed mechanisms for diverse functions. *Neuron*, *98*, 687–705. doi: 10.1016/j.neuron.2018.03.045.

Quintana, J., & Fuster, J. M. (1992). Mnemonic and predictive functions of cortical neurons in a memory task. *Neuroreport*, *3*, 721–724. doi: 10.1097/00001756-199208000-00018.

Rainer,.G, Rao,S. C., & Miller, E. K. (1999). Prospective coding for objects in primate prefrontal cortex. *J. Neurosci.*, *19*, 5493–5505. doi: 10.1523/JNEUROSCI.19-13-05493.

Rammsayer, T. H. (1994). Effects of practice and signal energy on duration discrimination of brief auditory intervals. *Percept. Psychophys.*, *55*, 454–464. doi: 10.3758/BF03205302.

Rigotti, M., Barak, O., Warden. M. R., Wang, X.-J., Daw, N. D., Miller, E. K., & Fusi, S (2013). The importance of mixed selectivity in complex cognitive tasks. *Nature*, *497*, 585–590. doi: 10.1038/nature12160.

Rose, G. J. (2014). Time computations in anuran auditory systems. *Front. Physiol.*, *5*, 206. doi: 10.3389/fphys.2014.00206.

Sadibolova, R., Sun, S., & Terhune, D. B. (2021). Using adaptive psychophysics to identify the neural network reset time in subsecond interval timing. *Exp. Brain Res.*, *239*, 3565–3572. doi: 10.1007/s00221-021-06227-0.

Shuler, M. G., & Bear, M. F. (2006). Reward timing in the primary visual cortex. *Science*, *311*, 1606–1609. DOI: 10.1126/science.1123513.

Spencer, R. M. C., Karmarkar, U., & Ivry, R. B. (2009). Evaluating dedicated and intrinsic models of temporal encoding by varying context. *Philos. Trans. R. Soc. Lond. B Biol. Sci.*, *364*, 1853–1863. doi: 10.1098/rstb.2009.0024.

Stokes, M. G. (2015). 'Activity-silent' working memory in prefrontal cortex: a dynamic coding framework. *Trends Cogn. Sci.*, *19*, 394–405. doi: 10.1016/j.tics.2015.05.004.

Tiganj, Z., Hasselmo, M. E., & Howard, M. W. (2015). A Simple biophysically plausible model for long time constants in single neurons. *Hippocampus*, *25*, 27–37. doi: 10.1002/hipo.22347.

Treisman, M. (1963). Temporal discrimination and the indifference interval: Implications for a model of the "internal clock". *Psychol. Monogr. Gen. Appl.*, *77*, 1–31. doi: 10.1037/h0093864.

van Ede, F., Niklaus, M., & Nobre, A. C. (2017). Temporal expectations guide dynamic prioritization in visual working memory through attenuated α oscillations. *J. Neurosci.*, *37*, 437–445. doi: 10.1523/JNEUROSCI.2272-16.2016.

Wang, X.-J. (2001). Synaptic reverberation underlying mnemonic persistent activity. *Trends Neurosci.*, *24*, 455–463. doi: 10.1016/S0166-2236(00)01868-3.

Xie, Y., Hu, P., Li, J., Chen, J., Song, W., Wang, X.-J., Yang, T., Dehaene,S., Tang, S., Min, B., & Wang, L. (2022). Geometry of sequence working memory in macaque prefrontal cortex. *Science*, *375*, 632–639. doi: 10.1126/science.abm0204.

Xu, M., Zhang, S.-y., Dan, Y., & Poo, M.-m. (2014), Representation of interval timing by temporally scalable firing patterns in rat prefrontal cortex. *Proc. Natl Acad. Sci.*, *111*:480–485. doi: 10.1073/pnas.1321314111.

Yang, G. R., Joglekar, M. R,. Song, H. F., Newsome, W. T., & Wang, X.-J. (2019) Task representations in neural networks trained to perform many cognitive tasks. *Nat. Neurosci.*, *22*, 297–306. doi: 10.1038/s41593-018-0310-2.

Yang, G. R., & Wang, X.-J. (2020). Artificial neural networks for neuroscientists: a primer. *Neuron*, *107*, 1048–1070. doi: 10.1016/j.neuron.2020.09.005.